

Chapter 60 - THE VSANS TECHNIQUE

Very small-angle neutron scattering (VSANS) pushes the SANS small-Q limit down by an order of magnitude. It consists in using tighter collimation and a higher resolution detector combined with the usual long flight paths and the use of a velocity selector. SANS collimation can be tightened in one of two ways: either through multiple circular converging apertures or through multiple slit converging collimation. This last option enhances flux-on-sample but introduces slit smearing. VSANS falls between regular SANS and Ultra SANS (USANS). The three major figures of merit (minimum Q, flux on sample, and Q resolution) are discussed for possible VSANS configurations for an instrument under construction at the NIST CNR.

1. MULTIPLE CIRCULAR CONVERGING COLLIMATION

Resolution

Multiple circular (also called pinhole) converging collimation is appealing because it allows an improvement in the resolution without too much loss in the flux on sample. Overkill apertures are required in order to eliminate neutron cross collimation.

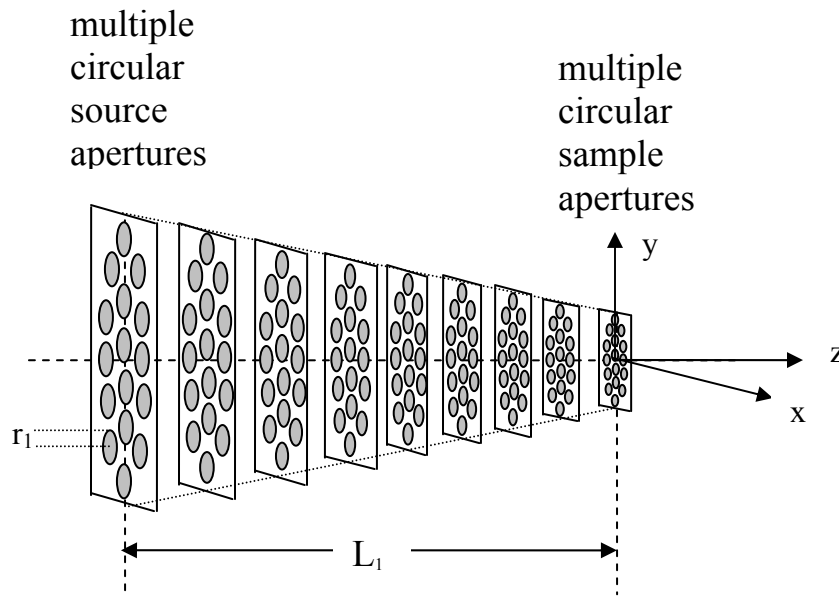


Figure 1: Multiple circular converging collimation. Intermediate apertures are placed to avoid cross collimation and keep neutrons in the same aperture channel. This figure is not to scale. Vertical scale is of order centimeters while horizontal scale is of order meters.

The main change to the variance of the Q resolution σ_Q^2 in going from a single large circular aperture to multiple small circular converging apertures is to **change** the radii of the source and sample apertures from **R_1 and R_2** (large radii) to **r_1 and r_2** (small hole radii) respectively. Everything else remains the same and will not be repeated here (Mildner-Carpenter, 1984; Mildner et al, 2005).

Similarly, the minimum scattering variable, Q_{\min} for the single aperture and multiple apertures collimations are the same provided that the small circular aperture radii are used.

Resolution with Focusing Lenses

The **addition of focusing lenses** to the multiple converging collimation geometry allows the opening up of the sample apertures without penalty in resolution. Modification of the Q resolution equations to incorporate lenses involves replacing the **sample aperture term**

$\left(\frac{L_1 + L_2}{L_1}\right) \frac{r_2^2}{4}$ by the following term $\frac{2}{3} \left(\frac{\Delta\lambda}{\lambda}\right)^2 \left(\frac{L_1 + L_2}{L_1}\right)^2 \frac{r_2^2}{4}$ where $\left(\frac{\Delta\lambda}{\lambda}\right)$ is the

wavelength spread and L_1 and L_2 are the source-to-sample and sample-to-detector distances. This corresponds to the condition where the neutron detector is located at the source image.

Similarly, modification of the **Q_{\min}** equations to incorporate lenses involves replacing the sample aperture term $\left(\frac{L_1 + L_2}{L_1}\right) r_2$ by the equivalent term $2 \left(\frac{\Delta\lambda}{\lambda}\right) \left(\frac{L_1 + L_2}{L_1}\right) r_2$.

Flux-on-Sample

The **neutron flux on sample** can be approximated by the following estimate (based on measurements made at the NG3 30 m SANS instrument at the NIST CNR).

$$\phi(\lambda) = \frac{1.507 * 10^{15}}{\lambda^4} \exp\left[-\frac{30.25}{\lambda^2}\right] \left(\frac{\Delta\lambda}{\lambda}\right) \frac{a_1}{L_1^2} \text{ n/cm}^2 \cdot \text{s.} \quad (1)$$

λ is the neutron wavelength, $\Delta\lambda$ is the wavelength spread, a_1 is the area of the source (small) aperture, and L_1 is the source-to-sample distance with $a_1 = \pi r_1^2$. The **neutron current** (or rate) **on sample** is given by:

$$\Phi(\lambda) = \phi(\lambda) a_2 = \frac{1.507 * 10^{15}}{\lambda^4} \exp\left[-\frac{30.25}{\lambda^2}\right] \left(\frac{\Delta\lambda}{\lambda}\right) \frac{a_1 a_2}{L_1^2}. \quad (2)$$

a_2 is the area of the sample aperture ($a_2 = \pi r_2^2$). For n small apertures, $\phi(\lambda)$ and $\Phi(\lambda)$ are multiplied by n .

Neutron Trajectories Constraint

Neutrons follow parabolic trajectories due to gravity. Neutrons climb up after crossing the source aperture, reach an apex half-way between the source and sample apertures, and fall back down to make it through the sample aperture. One constraint to consider for multiple circular converging collimation is the fact that all the neutron paths must make it through the overkill apertures, especially the middle overkill aperture. After the sample aperture, neutrons keep on falling down till they reach the detector plane.

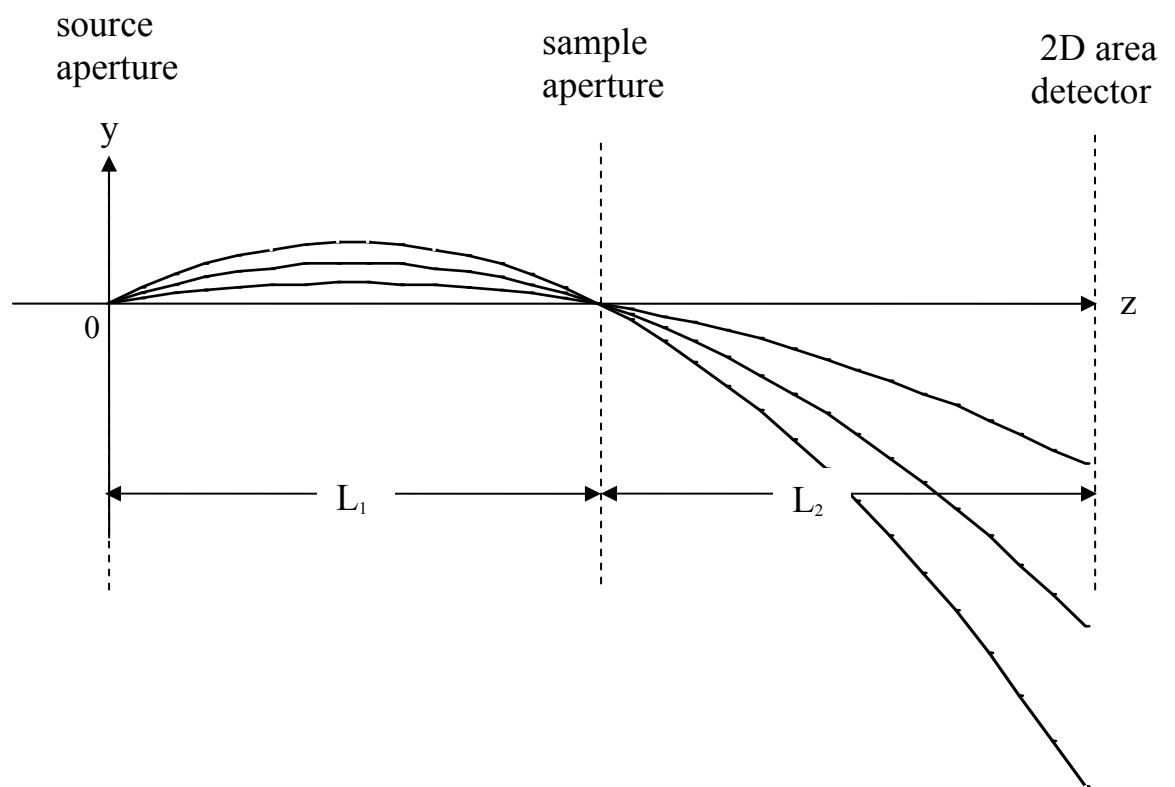


Figure 2: Trajectories of successfully transmitted neutrons corresponding to different wavelengths. Slower neutrons climb higher between the source and sample apertures.

Neutrons that are successfully transmitted through the source and sample apertures follow trajectories that depend on neutron wavelength. The maximum vertical beam spread occurs at mid-point between these two apertures. Neutrons follow parabolic trajectories that are described by the following parametric equation:

$$y(z) = [y(z)]_{\text{geo}} + [y(z)]_{\text{grav}} \quad (3)$$

$$[y(z)]_{\text{grav}} = -B\lambda^2(z^2 - zL_1).$$

with:

$$B = \frac{gm^2}{2h^2} = 3.073 * 10^{-9} \text{ cm}^{-1} \cdot \text{\AA}^{-2}. \quad (4)$$

Note that the related neutron fall constant at the detector location (i.e., for $z = L_1 + L_2$) is defined as:

$$A = L_2(L_1 + L_2) \frac{gm^2}{2h^2}. \quad (5)$$

The geometry part of the variance of the Q resolution corresponds to neutron trajectories without gravity effect. The effect of gravity is non-negligible for long wavelengths. The top neutron trajectory corresponds to $\lambda + \Delta\lambda$ whereas the bottom trajectory corresponds to $\lambda - \Delta\lambda$.

Constraining all neutrons within the wavelength spread to pass through the middle overkill aperture is performed by constraining the vertical neutron spread. The vertical beam spread corresponds to:

$$[\Delta y(z)]_{\text{grav}} = -B[(\lambda + \Delta\lambda)^2 - (\lambda - \Delta\lambda)^2](z^2 - zL_1) \quad (6)$$

$$= -B 4 \lambda^2 \left(\frac{\Delta\lambda}{\lambda} \right) (z^2 - zL_1).$$

And at the midpoint between the sample and source apertures (apex point where $z = L_1/2$), it is equal to:

$$[\Delta y(L_1/2)]_{\text{grav}} = B\lambda^2 \left(\frac{\Delta\lambda}{\lambda} \right) L_1^2. \quad (7)$$

The constraint that all neutrons within the wavelength spread make it through the middle overkill aperture (located at $z = L_1/2$) can be stated as:

$$2r_m \geq [\Delta y(L_1/2)]_{\text{geo}} + [\Delta y(L_1/2)]_{\text{grav}}. \quad (8)$$

r_m is the radius of the middle overkill aperture. This constraint translates to the condition:

$$r_m \geq \frac{r_1 + r_2}{2} + \frac{B\lambda^2 L_1^2}{2} \left(\frac{\Delta\lambda}{\lambda} \right). \quad (9)$$

This is a constraint on the size of the middle overkill aperture r_m in terms of the radii of the source and sample apertures r_1 and r_2 , the source-to-sample distance L_1 , the neutron wavelength λ and wavelength spread $\Delta\lambda$. An alternative criterion (not considered here) could be to constrain the variance of the beam spread instead.

2. SPECIFIC CASE OF MULTIPLE CIRCULAR CONVERGING COLLIMATION

Without Lenses

Consider the following possible VSANS instrumental conditions:

$$\begin{aligned} \text{Source circular aperture (hole) radius: } r_1 &= 0.3 \text{ cm} & (10) \\ \text{Sample circular aperture (hole) radius: } r_2 &= 0.15 \text{ cm} \\ \text{Number of apertures (holes): } n &= 18 \\ \text{Detector cell horizontal size: } \Delta x_3 &= 0.1 \text{ cm} \\ \text{Detector cell vertical size: } \Delta y_3 &= 0.1 \text{ cm} \\ \text{Source-to-sample distance: } L_1 &= 20 \text{ m} \\ \text{Sample-to-detector distance: } L_2 &= 20 \text{ m} \\ \text{Neutron wavelength: } \lambda &= 8.5 \text{ \AA} \\ \text{Wavelength spread: } \frac{\Delta\lambda}{\lambda} &= 0.13. \end{aligned}$$

This corresponds to a source aperture of 15 cm * 6 cm and a sample aperture (and a sample size) of 7.5 cm * 3 cm.

Therefore $A = 0.0246 \text{ cm}/\text{\AA}^2$ so that $\sigma_x^2 = \sigma_y^2 = 0.0458 \text{ cm}^2$ and:

$$\begin{aligned} \sigma_{Q_x}^2 &= 6.26 * 10^{-9} + 0.0028 Q_x^2 \text{ (in units of } \text{\AA}^{-2}) & (11) \\ \sigma_{Q_y}^2 &= 1.11 * 10^{-8} + 0.0028 Q_y^2 \text{ (in units of } \text{\AA}^{-2}). \end{aligned}$$

For this multiple circular converging collimation configuration,

$$\begin{aligned} Q_{\min}^x &= 0.00024 \text{ \AA}^{-1} & (12) \\ Q_{\min}^y &= 0.00041 \text{ \AA}^{-1}. \end{aligned}$$

Neutrons fall by 1.78 cm in the detector plane ($z = L_1 + L_2$). At the apex position ($z = L_1/2$), neutron height corresponds to $y(L_1/2) = 0.22 \text{ cm}$. This is the amount by which the

middle overkill aperture has to be raised. Other overkill apertures are raised proportionally.

It is noted that a VSANS instrument with multiple circular converging collimation operates at preset discrete wavelengths because each wavelength requires different height adjustments for the overkill apertures. Based on the constraint criterion used, the middle overkill aperture must have a radius of $r_m \geq 0.283$ cm for $\lambda = 8.5$ Å.

The neutron flux and count rate on sample are estimated for a neutron wavelength and wavelength spread of $\lambda = 8.5$ Å and $\Delta\lambda/\lambda = 0.13$. Using the source and sample areas of $a_1 = 0.283$ cm² and $a_2 = 0.0707$ cm², and $n = 18$, one obtains:

$$\begin{aligned}\phi(8.5 \text{ \AA}) &= 31,400 \text{ n/cm}^2.\text{s} \\ \Phi(8.5 \text{ \AA}) &= 2,218 \text{ n/s.}\end{aligned}\tag{13}$$

These numbers are for a possible VSANS configuration characterized by a Q_{\min} which is an order of magnitude lower than the similar SANS configuration.

With Lenses

When using focusing lenses, the sample aperture can be opened up. Consider now $r_2 = 0.5$ cm. This gives slightly lower resolution:

$$\begin{aligned}\sigma_{Q_x}^2 &= 3.57 * 10^{-9} + 0.0028 Q_x^2 \text{ (in units of \AA}^{-2}\text{)} \\ \sigma_{Q_y}^2 &= 8.43 * 10^{-9} + 0.0028 Q_y^2 \text{ (in units of \AA}^{-2}\text{)}.\end{aligned}\tag{14}$$

$$\begin{aligned}Q_{\min}^x &= 0.00022 \text{ \AA}^{-1} \\ Q_{\min}^y &= 0.00040 \text{ \AA}^{-1}.\end{aligned}$$

The neutron current is higher since the source aperture is larger.

$$\begin{aligned}\phi(8.5 \text{ \AA}) &= 31,400 \text{ n/cm}^2.\text{s} \\ \Phi(8.5 \text{ \AA}) &= 24,649 \text{ n/s.}\end{aligned}\tag{15}$$

Use MgF₂ lenses (one stack of lenses per small aperture) and recall the following basic equations for MgF₂ lenses:

$$\frac{N\lambda^2}{R} \left(\frac{L_1 L_2}{L_1 + L_2} \right) = \frac{\pi}{\rho b_c} = 6.25 * 10^5 \text{ \AA}^2.\tag{16}$$

Consider lenses of radius of curvature R that are thin at the center (0.5 mm thickness) in order to keep neutron transmission high. A multiple aperture configuration with $L_1 = L_2 = 20$ m yields a focal length of:

$$f = \left(\frac{L_1 L_2}{L_1 + L_2} \right) = 1000 \text{ cm} . \quad (17)$$

Therefore:

$$\frac{N\lambda^2}{R} = 625 \text{ \AA}^2 . \quad (18)$$

For $R = 0.5 \text{ cm}$ and $\lambda = 8.5 \text{ \AA}$, it takes about 4.33 lenses to achieve the desired focal length.

In order to enhance flux-on-sample, multiple-slit converging collimation is discussed next.

3. MULTIPLE SLIT CONVERGING COLLIMATION

Multiple slit converging collimation has the advantage of increasing flux on sample by opening up the vertical resolution while tightening the horizontal resolution. The effect of gravity becomes irrelevant.

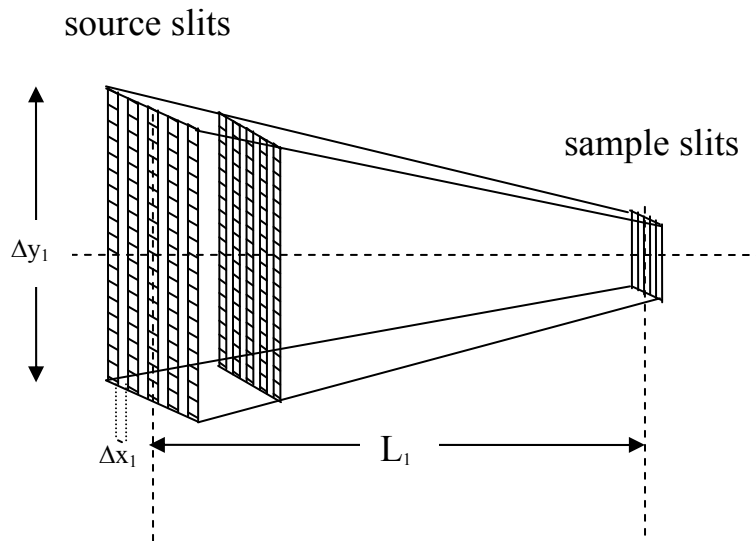


Figure 3: Multiple converging slit collimation. Intermediate apertures are placed so as to avoid cross collimation and keep neutrons in the same aperture channel.

The Q resolution for multiple slit converging collimation is similar to that for multiple circular converging collimation but with different “geometry” contributions σ_x^2 and σ_y^2 .

Also, the averages $\langle x^2 \rangle_1$ and $\langle x^2 \rangle_2$ over the beam defining apertures for slits are different from those for circular apertures. Recall that:

$$\langle x^2 \rangle_1 = \frac{1}{3} \left(\frac{\Delta x_1}{2} \right)^2 \text{ for slit of width } \Delta x_1 \quad (19)$$

$$\langle x^2 \rangle_1 = \frac{R_1^2}{4} \text{ for circular aperture of radius } R_1$$

Similarly, the Q_{\min} value for multiple converging slit collimation in the horizontal (x-) direction is the same as that for multiple circular converging collimation. The same expression for the flux-on-sample applies for multiple circular collimation and multiple slit collimation.

4. PERFORMANCE OF THE VARIOUS VSANS CONFIGURATIONS

Comparison of the performance of various VSANS configurations for circular or slit apertures with or without lenses is presented in a table. These predictions assume the following:

- Source-to-sample distance: $L_1 = 20$ m
- Sample-to-detector distance: $L_2 = 20$ m
- Neutron wavelength: $\lambda = 8.5$ Å
- Wavelength spread: $\frac{\Delta\lambda}{\lambda} = 0.13$.
- Source aperture of 15 cm * 6 cm
- Sample aperture (and sample size) of 7.5 cm * 3 cm.

Table 1: Prediction of the performance of the VSANS instrument for various configurations

| | Circular Apertures | | Slit Apertures | |
|----------------|---|---|--|---|
| | Small Aperture Sizes (cm) | Performance | Small Slit Sizes (cm) | Performance |
| Without Lenses | $r_1 = 0.3$ $r_2 = 0.15$ $n = 18$ | $Q_{\min}^X = 0.00024 \text{ \AA}^{-1}$ $Q_{\min}^Y = 0.00041 \text{ \AA}^{-1}$ $\phi(8.5 \text{ \AA}) = 31,400 \text{ n/cm}^2 \cdot \text{s}$ $\Phi(8.5 \text{ \AA}) = 2,218 \text{ n/s}$ | $\Delta x_1 = 0.6$ $\Delta y_1 = 15$ $\Delta x_2 = 0.3$ $\Delta y_2 = 7.5$ $n = 3$ | $Q_{\min}^X = 0.00024 \text{ \AA}^{-1}$ $Q_{\min}^Y = 0.0057 \text{ \AA}^{-1}$ $\phi(8.5 \text{ \AA}) = 1.67 * 10^5 \text{ n/cm}^2 \cdot \text{s}$ $\Phi(8.5 \text{ \AA}) = 3.75 * 10^5 \text{ n/s}$ |
| With Lenses | $r_1 = 0.3$ $r_2 = 0.5$ $n = 18$ | $Q_{\min}^X = 0.00022 \text{ \AA}^{-1}$ $Q_{\min}^Y = 0.00040 \text{ \AA}^{-1}$ | $\Delta x_1 = 0.6$ $\Delta y_1 = 15$ $\Delta x_2 = 1.0$ | $Q_{\min}^X = 0.00022 \text{ \AA}^{-1}$ $Q_{\min}^Y = 0.0037 \text{ \AA}^{-1}$ $\phi(8.5 \text{ \AA}) = 1.67 * 10^5 \text{ n/cm}^2 \cdot \text{s}$ |

| | | | | |
|--|--|--|-------------------------------|---|
| | | $\phi(8.5 \text{ \AA})=31,400 \text{ n/cm}^2\cdot\text{s}$ $\Phi(8.5 \text{ \AA}) = 24,649 \text{ n/s}$ | $\Delta y_2 = 7.5$ $n = 3$ | $\Phi(8.5 \text{ \AA}) = 1.25 \cdot 10^6 \text{ n/s}$ |
|--|--|--|-------------------------------|---|

The configuration for circular apertures with lenses yields a slightly lower Q_{\min}^x . This Q_{\min}^x is maintained when moving to slit collimation in the horizontal direction. Using lenses increases the neutron current. Using slits enhances the flux-on-sample. This, however, requires dealing with slit smearing corrections. Note that the neutron flux on sample and neutron current were estimated based on predictions for the NG3 guide.

The two main figures of merit (variance of the Q resolution and Q_{\min}) are compared in a figure.

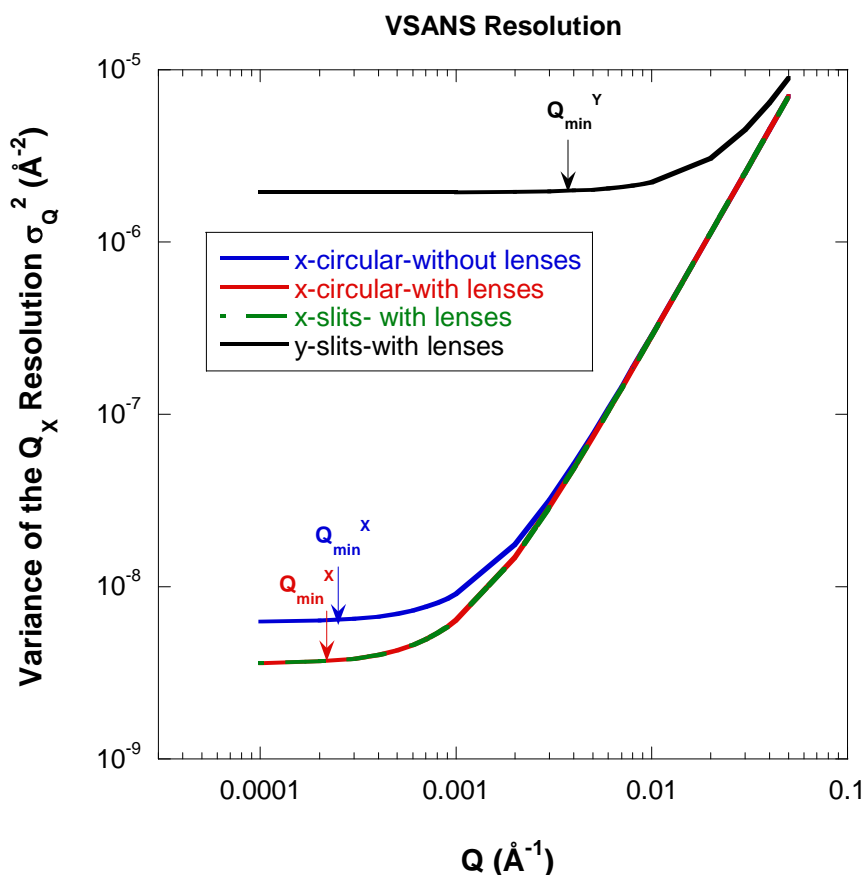


Figure 4: Variation of the variance of the Q_x resolution and Q_{\min} for various VSANS configurations. The x- and y- axes are along the horizontal and vertical directions (the z-direction is along the neutron beam).

5. OVERKILL APERTURES

Spacing Scheme

Uniformly spacing the overkill apertures is not the most effective way of distributing them. Another scheme is discussed here. A similar scheme has been used to place disks on multidisk velocity selectors.

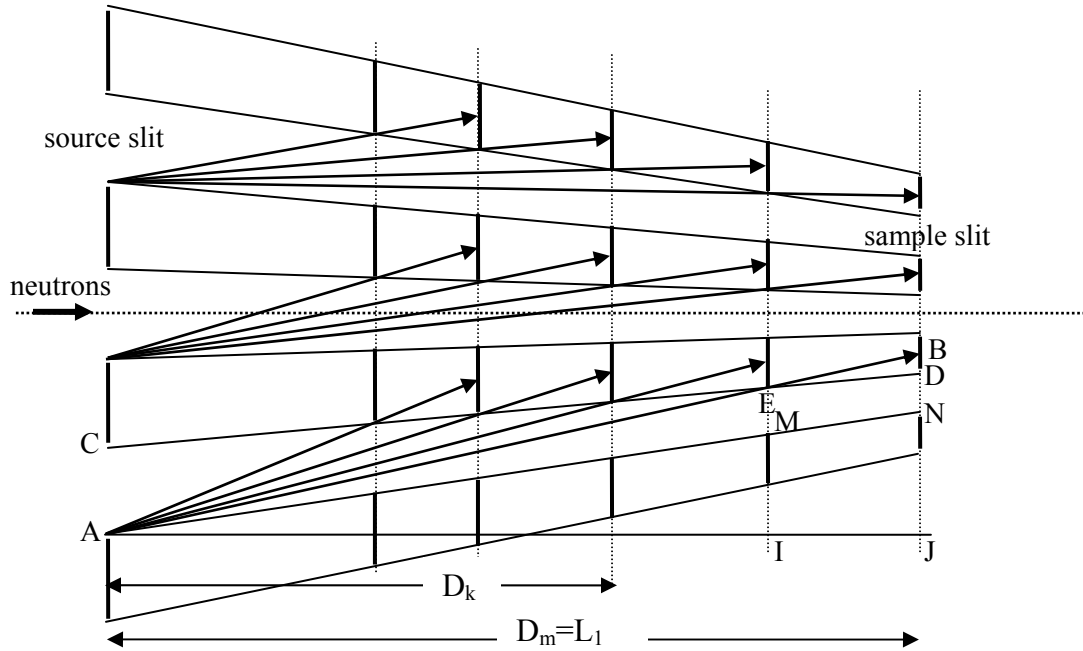


Figure 5: Top view of the **distribution scheme** proposed to place the overkill apertures along the neutron path. The neutron source aperture is located on the left and the sample aperture is located on the right.

The proposed scheme is illustrated in a figure. It consists in placing a series of m overkill apertures starting from the sample aperture on the right side. A line AB is drawn to the middle of an absorbing region. It cuts line CD at a point E. This gives the location of aperture $m-1$ a distance D_{m-1} from the source aperture (left side).

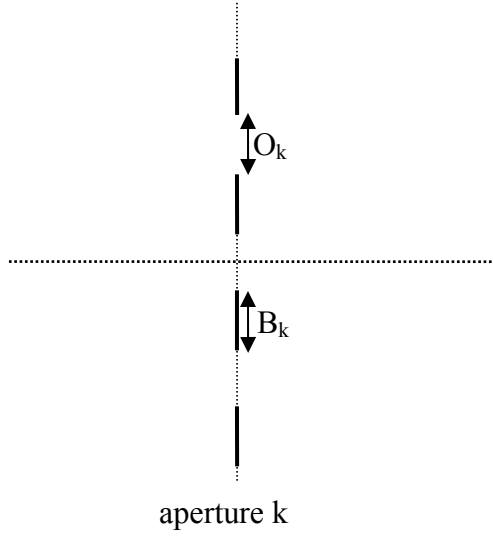


Figure 6: Open slits and blocked regions on aperture k.

Defining the sizes of the open (slit) and of the blocked parts of aperture k as O_k and B_k respectively, one can express the blocked-to-open ratio as:

$$w = \frac{B_m}{O_m} = \frac{B_k}{O_k} . \quad (20)$$

The distance D_{m-1} can be calculated from distance D_m based on a scaling argument but working backward.

$$\frac{D_{m-1}}{D_m} = \frac{AI}{AJ} = \frac{IE}{JB} = \frac{ME}{NB} = \frac{O_{m-1}}{O_m + \frac{B_m}{2}} = \frac{O_{m-1}}{O_m} \frac{1}{1 + \frac{w}{2}} \quad (21)$$

$$D_{m-1} = D_m \frac{O_{m-1}}{O_m} K$$

Where:

$$K = \frac{1}{1 + \frac{w}{2}} . \quad (22)$$

D_m is the full source-to-sample distance (usually referred to as L_1). Similarly, one obtains for the location of subsequent slits:

$$D_{m-2} = D_m \left(\frac{O_{m-2}}{O_m} \right) K^2 \quad (23)$$

The general formula is:

$$D_{m-k} = D_m \left(\frac{O_{m-k}}{O_m} \right) K^k. \quad (24)$$

The position of overkill apertures follows a geometric progression. This scheme ensures that no unwanted open channels are left open and guarantees more than single coverage of the blocked channels. In practice this scheme is used for a reasonable number of overkill slits.

The transmission factor for the apertures is given by:

$$T = \left(\frac{1}{1+w} \right) \quad (25)$$

Slit Sizes

The following scaling relation applies:

$$\frac{O_{m-1}}{O_m} = \frac{O_1(D_m - D_{m-1}) + O_m D_{m-1}}{O_m D_m}. \quad (26)$$

O_1 is the slit (open) size of the first (source) aperture and O_m is the slit (open) size of the last (sample) aperture. Replacing $D_{m-1} = D_m \left(\frac{O_{m-1}}{O_m} \right) K$, one obtains the following slit sizes relationship:

$$O_{m-1} = \frac{O_1}{1 + K \frac{O_1 - O_m}{O_m}}. \quad (27)$$

Furthermore:

$$O_{m-k} = \frac{O_1}{1 + K^k \frac{O_1 - O_m}{O_m}}. \quad (28)$$

This scheme would work for multiple slit converging apertures as well. For multiple circular converging apertures, vertical apertures sizes would have to be corrected for the gravity effect using the constraint discussed previously.

6. SPECIFIC CASE FOR OVERKILL APERTURES

Consider the following specific case for converging circular apertures without lenses.

Slit opening on the source aperture $O_1 = 0.6$ cm.
Blocked area between slits on the source aperture $B_1 = 0.6$ cm.
Slit opening on the sample aperture $O_m = 0.3$ cm.
Blocked area between slits on the sample aperture $B_m = 0.3$ cm.
Source-to-sample distance $D_m = 20$ m.
Consider $m = 9$; i.e., a total of 9 apertures.

In this case:

Blocked-to-open ratio $w = 1$.
Apertures transmission $T = 1/2 = 50\%$.
Factor $K = 2/3 = 0.667$
Factor $\frac{O_1 - O_m}{O_m} = 1$.

The apertures are located at the following distances from the source aperture:

$D_9 = 20$ m (sample aperture)
 $D_8 = 16.00$ m
 $D_7 = 12.32$ m
 $D_6 = 9.15$ m
 $D_5 = 6.61$ m
 $D_4 = 4.66$ m
 $D_3 = 3.24$ m
 $D_2 = 2.22$ m
 $D_1 = 0$ m (source aperture).

This is a possible placement sequence for the collimation apertures. This sequence can be used either in the forward or backward directions starting from the neutron source aperture.

Slit sizes in each aperture are as follows:

$O_9 = 0.30$ cm (sample aperture slit).
 $O_8 = 0.36$ cm
 $O_7 = 0.42$ cm
 $O_6 = 0.46$ cm

$O_5 = 0.50$ cm
 $O_4 = 0.53$ cm
 $O_3 = 0.55$ cm
 $O_2 = 0.57$ cm
 $O_1 = 0.6$ cm (source aperture slit).

This is a possible sequence of slit sizes on the apertures.

7. SCATTERING ANGLE FOR MULTIPLE CONVERGING COLLIMATION

An issue worth discussing is whether the scattering angle would be the same for the various neutron scattering rays involved in the multiple converging collimation. As shown graphically, all of the marked scattering angles are equal within the first order (small-angle) approximation. Higher order corrections may be needed when scattering angles are not small.

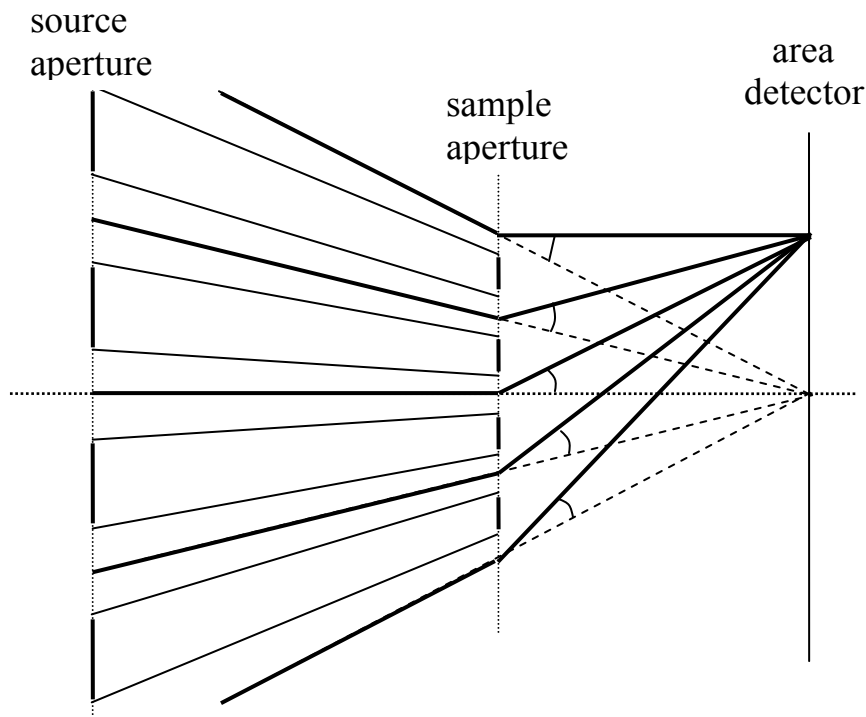


Figure 7: The marked angles are all equal to the scattering angle θ within the first order (small-angle) approximation.

8. DISCUSSION

The VSANS instrument combines the VSANS and SANS measurement ranges chosen in turn. Use of single-aperture collimation and coarse detector resolution covers the standard SANS range. Insertion of multiple apertures and of the high resolution neutron detector

covers the VSANS range. The use of focusing lenses tightens the neutron beam spot on the detector while opening up the sample aperture. The use of multiple slits helps increase the neutron current substantially. This feature, however, works best with taller (rectangular) samples.

The VSANS instrument will use a couple of discrete wavelengths (for example 6 Å and 8.5 Å). These wavelengths must be higher than the Bragg cutoff (around 5 Å) for MgF₂ used for focusing lenses.

The VSANS instrument will use a “regular” area detector with resolution around 5 mm. A row of linear position sensitive detectors may replace the area detector or complement it by covering the larger angle areas. Linear “tube” detectors have the advantage of high count rate and robustness. Banks of such tube detectors could be placed on both sides of the main detector as well as at the top and bottom. This would cover a wide area.

The VSANS option requires a high resolution neutron detector as well. The technology for building high resolution (1 mm or 2 mm) detectors is improving. The Millimeter-resolution Large Area Neutron Detectors (MILAND) project is an international focus group for improving such technology. Imaging plates and scintillation detectors can achieve that resolution. Imaging plates are sensitive to gammas and scintillation detectors can produce undesired gamma background.

The lens system for multiple slits could be designed by incorporating holes in a slab cassette.

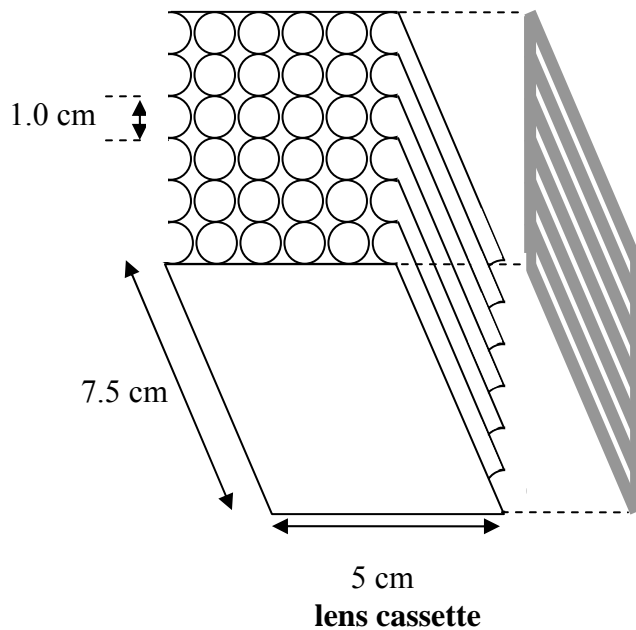


Figure 8: Schematic representation of the vertical lenses cassette that would comprise a number of slits. The cassette consists essentially of a slab with equally spaced vertical

holes that are lined up. Two half holes make up one row of lenses, two half holes and four full holes in-between make up five rows of lenses.

The VSANS instrument would benefit from the use of two velocity selectors, one with typical and the other with high resolution respectively.

Two Velocity Selectors

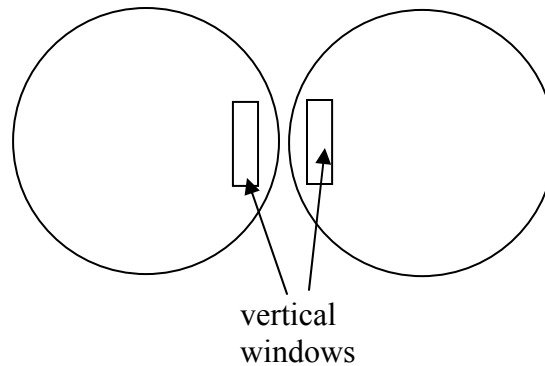


Figure 9: Two velocity selectors can be used, one characterized by $\Delta\lambda/\lambda \sim 0.15$ and the other one with $\Delta\lambda/\lambda \sim 0.05$.

Typical low-Q and high-Q configurations cover the following SANS Q range: $0.003 \text{ \AA}^{-1} < Q < 0.3 \text{ \AA}^{-1}$. The USANS Q range is typically $3 \cdot 10^{-5} \text{ \AA}^{-1} < Q < 0.005 \text{ \AA}^{-1}$. A figure shows SANS and USANS data taken from 4 % poly(ethylene oxide) in d-ethanol. USANS requires high scattering cross section samples. The SANS data were acquired over a period of 30 minutes and the USANS data were acquired over a period of 5 hours. At the very low-Q, USANS statistics are very good, but for $Q > 0.0004 \text{ \AA}^{-1}$, the USANS statistics become poor. This is where VSANS will improve data quality (counting statistics) in that region. The VSANS instrument will cover the Q range $3 \cdot 10^{-4} \text{ \AA}^{-1} < Q < 0.009 \text{ \AA}^{-1}$. The NIST CNR VSANS instrument is under construction (Barker, 2007). **A VSANS instrument was built and is under operation at Saclay** (Brulet et al, 2008).

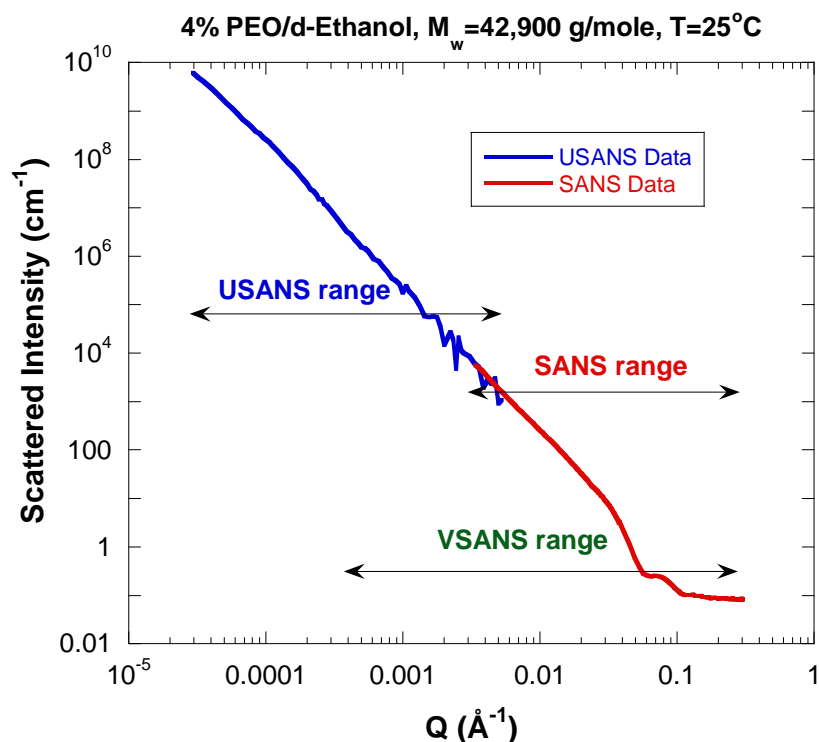


Figure 10: Compound plot of **SANS data and USANS data** from a 4 % poly(ethylene oxide) sample in d-ethanol. The Q range of the proposed VSANS technique is shown.

REFERENCES

- D.F.R. Mildner, and J.M. Carpenter, "Optimization of the Experimental Resolution for SAS", *J. Appl. Cryst.* **17**, 249-256 (1984).
- D.F.R. Mildner, B. Hammouda, and S.R. Kline, "A Refractive Focusing Lens System for SANS", *J. Appl. Cryst.* **38**, 979-987 (2005).
- J.G. Barker, "VSANS Conceptual Design Report", NIST Center for Neutron Research Internal Report (2007)
- A. Brulet, V. Thevenot, D. Lairez, S. Lecommandoux, W. Agut, S.P. Armes, J. Du and S. Desert, "Toward a New Lower Limit for the Minimum Scattering Vector on the VSANS Spectrometer at Laboratoire Leon Brillouin", *J. Appl. Cryst.* **41**, 161-166 (2008).

QUESTIONS

1. What are the main components that make VSANS possible?
2. What is the main difference in the variance of the resolution function for circular and slit apertures?
3. What term changes in the variance of the resolution function when using focusing lenses?
4. What is the modification of the sample term in Q_{\min} when using focusing lenses?
5. Why is the VSANS option with multiple slits characterized by so much higher neutron current? What is the main drawback of using slit collimation?
6. What type of detectors could achieve 1 mm to 2 mm spatial resolution?

ANSWERS

1. The main components that make VSANS possible are: tight collimation through the use of multiple apertures and high resolution detector.
2. The main difference in the variance of the resolution function is in the averaging of the geometry contribution, $\langle x^2 \rangle_1 = R_1^2/4$ for a circular aperture of radius R_1 whereas $\langle x^2 \rangle_1 = (\Delta x_1/2)^2/3$ for a slit of width Δx_1 .
3. The only term that changes in the variance of the resolution function is the sample aperture term which involves $\langle x^2 + y^2 \rangle_2$. When using focusing lenses, this term is reduced; i.e., it is multiplied by the term $(2/3)(\Delta\lambda/\lambda)^2$ which is small.
4. The sample term in Q_{\min} is multiplied by $2(\Delta\lambda/\lambda)$ when using focusing lenses.
5. The VSANS option with multiple slits is characterized by a much higher neutron current because collimation is opened up in the vertical direction. The main drawback of this is slit smearing of the data.
6. Imaging plates and scintillators could achieve sub-millimeter spatial resolution. These, however, are characterized by gamma background issues.